Early Results and Validation of SAGE III-ISS Ozone Profile Measurements from Onboard the International Space Station

M. Patrick McCormick[1], Liqiao Lei[1], Michael T. Hill[1], John Anderson[1], Richard Querel[2], and Wolfgang Steinbrecht[3]

[1]Center for Atmospheric Sciences, Department of Atmospheric and Planetary Sciences, Hampton University, Hampton, VA, 23668, USA

[2]National Institute of Water & Atmospheric Research (NIWA), Lauder, New Zealand

[3]Deutscher Wetterdienst, Hohenpeissenberg, Germany

Corresponding to: M. Patrick McCormick (pat.mccormick@hamptonu.edu)

Abstract. The Stratospheric Aerosol and Gas Experiment III (SAGE III) instrument, was launched on February 19, 2017 from the NASA Kennedy Space Center, and integrated aboard the International Space Station (ISS). SAGE III-ISS has been providing ozone profile measurements since June 2017. This paper presents an early validation of the Level 2 solar and lunar occultation ozone data products using ground-based lidar and ozonesondes from Hohenpeissenberg and Lauder and satellite ozone vertical products from the Atmospheric Chemistry Experiment Fourier-Transform Spectrometer (ACE-FTS) instrument. Average differences in ozone concentration between SAGE III-ISS and Hohenpeissenberg lidar observations for one year are less than 10% between 16 and 42 km and less than 5% between 20 and 40 km. Hohenpeissenberg ozonesonde comparisons are mostly within 10% between 18 and 30 km. The Lauder lidar comparison results are less than 10% between 17 and 37 km, and less than 10% between 19 km and 31 km for Lauder ozonesondes. The seasonal average differences of ozone concentration between SAGE III-ISS and ACE-FTS are mostly less than 5% between 20 and 45 km for both the Northern and Southern Hemispheres. All results from these comparisons show that the SAGE III-ISS ozone solar data compare well with correlative measurements throughout the stratosphere. With few comparisons available, the percentage difference between the SAGE III-ISS lunar ozone data and the ozonesonde data is less than 10% between 19 and 27 km. The percentage difference between the SAGE III-ISS lunar ozone data and the ACE-FTS ozone data is less than 10% between 20 and 40 km.

1. Introduction

Ozone plays a significant role in the atmosphere because it contributes to the radiative balance of the atmosphere by absorbing ultraviolet (UV) solar radiation, and, in addition affects the health of humans, animals, and plants (Solomon, 1999). Therefore, it is important to understand its global variations and trends (McCormick et al., 1992; Reinsel et al., 2002; Bourassa et al., 2014; Harris et al., 2015), and its impact on climate change (Rex et al, 2004; Son et al., 2008; Thompson et al, 2011). In addition, by modifying the Brewer-Dobson Circulation and stratospheric temperatures, climate change impacts global ozone concentrations (Weber et al. 2018). Ozone measurements from the SAGE series of satellite instruments, including SAGE I, II, III/METEOR-3M, and III/ISS, provide important data to investigate stratospheric change and long-term variability in the vertical distribution of stratospheric ozone. The occultation technique that the SAGE series utilizes provides a consistent methodology and fundamental assumption for processing data (McCormick et al., 1989; Wang et al., 2006; Damadeo et al., 2013). The solar occultation method makes SAGE one of the best series of satellite instruments for high resolution stratospheric ozone measurements. Other than the SAGE series, previous solar occultation satellite instruments include the HALogen Occultation Experiment (HALOE) (Russell et al., 1993), Polar Ozone and Aerosol Measurement III (Lucke et al., 1999), and Atmospheric

Chemistry Experiment Fourier Transform Spectrometer (ACE-FTS) (Bernath et al., 2005). The Scanning Imaging Absorption spectrometer for atmospheric ChartographY (SCIAMACHY) also has an occultation mode (Bovensmann et al., 1999). The ACE-FTS is still in operation and is providing valuable data for the SAGE III-ISS validation as is shown in this paper. It is important for the SAGE III-ISS ozone profiles to be well validated to extend the long-standing ozone record of observations from the SAGE series, POAM III, HALOE, and ACE-FTS. The well characterized ozone data will contribute to the investigation of any trend and possible ozone recovery due to a reduction in Chlorofluorocarbons (CFC). In this paper, the global SAGE III-ISS ozone profile data are compared with correlative datasets to investigate possible differences. These comparisons begin the process of showing that SAGE III-ISS ozone data can be used for scientific studies. A systematic assessment of the early SAGE III-ISS ozone profiles is conducted with observations made by comparing SAGE III-ISS ozone profiles with ozone profiles made by Hohenpeissenberg and Lauder ground-based lidar and ozonesondes, as well as satellite data from the ACE-FTS. Section 2 describes the instrument and ozone product for the comparison, as well as the criteria for coincidence and the methodology for validation. The comparison results between coincident events are shown in Sect. 3. The overall summary and conclusion are presented in Sect. 4.

2. Instruments and Methods

2.1 SAGE III-ISS

The SAGE III-ISS payload was launched by the SpaceX Falcon rocket on 19 February 2017 from the NASA Kennedy Space center and delivered to the ISS by the SpaceX Dragon spacecraft. It was mated to the ISS on 7 March 2017. The ISS is flying in a 51.64° inclination low-Earth orbit, which provides low- and mid-latitude occultation coverage. Figure 1 shows SAGE III-ISS solar and lunar occultation coverage from June 2017 to November 2018. The primary objective of the SAGE III-ISS mission is to obtain vertical profiles of ozone, water vapor, nitrogen dioxide, nitrogen trioxide, and aerosol extinction at multiple wavelengths, using solar and lunar occultation measurements. Similar to the SAGE III/METEOR-3M, SAGE III-ISS uses an 809×10 pixel Charged Couple Device (CCD) array to provide continuous spectral coverage from 280-1040 nm with a spectral resolution of 1 to 2 nm. Additionally, an InGaAs infrared (IR) photodiode centered at 1550 nm is included for aerosol extinction measurements at a longer wavelength (Wang et al., 2006). Only 87 pixel groups are transmitted from the satellite for gaseous species and aerosol retrieval because of the limitation in the telemetry bandwidth. As well as solar occultation, SAGE III-ISS is capable of making lunar occultation measurements at nighttime for ozone, nitrogen dioxide, nitrogen trioxide, and chlorine dioxide. SAGE III-ISS level 2 solar species retrievals include three ozone profile products.
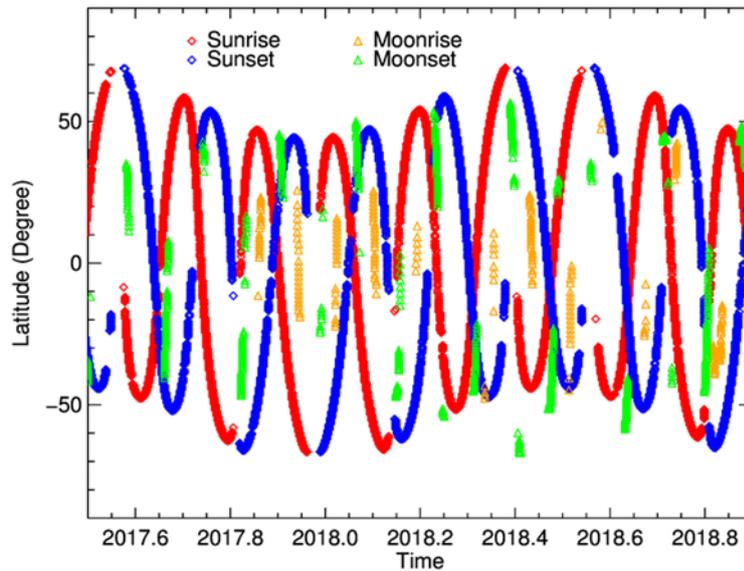
Figure 1. The SAGE III-ISS solar and lunar occultation coverage from June 2017 to November 2018. The red curves show the sunrise events; the blue curves show the sunset events; the orange curves show the moon rise events and the green curves show the moonset events.

The profile based upon the measurement made in the Hartley-Huggins band is denoted as Mesospheric ozone (MesO3). The profile based upon measurements in the Chappuis band is denoted as Multiple Linear Regression Ozone (ChapO3). The profile obtained using a similar approach to that used by SAGE II is denoted as Least Squares Ozone (Ozone_aO3) [SAGE III-ISS Data Products User's Guide: https://eosweb.larc.nasa.gov/project/sageiii-iss/guide/DPUG-G3B-2-0.pdf; Damadeo et al., 2013]. The version 5.1 Least Squares Ozone profile is used here for ozone comparison between the SAGE III-ISS and correlative measurements. The vertical resolution of the SAGE III-ISS ozone profiles is 0.5 km altitude.

2.2 Lidar and Ozonesonde

Lidar and ozonesonde ozone profiles provided by the Network for the Detection of Atmospheric Composition Change (NDACC) are used for SAGE III-ISS ozone profile comparisons. An NDACC station at mid-latitude in each hemisphere (Hohenpeissenberg in the Northern Hemisphere and Lauder in the Southern Hemisphere) with an established record of regular ozone measurements from both lidars and sondes is selected for the initial validation. Future validation efforts will include other stations. The Hohenpeissenberg (48° N, 11° E) ozone lidar has been providing ozone profile data from 15 to 50 km since 1987. The Hohenpeissenberg balloon ozonesonde has been providing ozone profile data since 1967. A remote-sensing research station located at Lauder, New Zealand (45° S, 169.7° E) has been providing lidar ozone profile data from 8 to 50 km since 1994 and ozonesonde ozone profiles data from 0 to 32 km since 1986.

During the first year of SAGE III-ISS observations (June 2017 to May 2018), ozonesonde launches were conducted at Hohenpeissenberg generally 2-3 times per week with the greater frequencies occurring in the October to April time frame. Ozonesonde launches at Lauder were conducted mostly 3-5 times per month during the year with exceptions in June (2 measurements) and October (6 measurements). Lidar measurements at Hohenpeissenberg were made 6-9 times per month in 2017 and 4-6 times per month in 2018, except for April in which 11 measurements were made. Lidar measurements at Lauder were made 1-4 times per month during the year. For details see the NDACC website (www.ndaccdemo.org/stations).

Typical uncertainties in ozone measurements from the Hohenpeissenberg Brewer-Mast sondes are better than 5% near the ozone maximum at ~40 hPa and increase to values of 10% or more above 10 hPa (~30 km) and up to 15%

in the troposphere (Kerr et al., 1994; SPARC 1998). Estimated uncertainties in ozone profiles derived from the
Lauder ECC sondes are generally better than 5% in the troposphere and stratosphere up to 10 hPa (~30 km) and up to 10% at higher altitudes (Bodeker et al., 1998). Uncertainties in ozone measurements from the lidar systems are typically 5% or better between 15 and 35 km altitude and less than 10% up to about 40 km altitude (Leblanc et al., 2016).

2.3 ACE-FTS

The Canadian Atmospheric Chemistry Experiment (ACE) on the SCISAT-1 satellite was launched on 12 August 2003 (Bernath et al., 2005) and is operational at the time of this writing. The ACE-FTS is one of the two instruments on-board the spacecraft and provides vertical profiles of ozone and trace gases, as well as temperature, pressure, and aerosol extinction (Boone et al., 2005, Waymark et al., 2013). ACE-FTS makes its solar occultation measurements in the 85°S to 85°N latitude region due to its circular 650 km, 74° inclination, low-Earth orbit (Bernath et al., 2005). The ACE-FTS vertical measurement range typically extends from 10-95 km for ozone. The maximum vertical resolution of ACE-FTS is 3-4 km based on its instrument field-of-view (Dupuy et al., 2009). ACE-FTS level 2 version 3.5/3.6 data are used for the ozone comparisons in this work.

2.4 The Methodology for Comparisons

As a satellite with near-global coverage, SAGE III-ISS allows for a significant number of coincidences with data from correlative instruments, which is expected to yield reliable conclusions regarding the consistencies of its data (Imai, 2013). Coincident ozone profiles from SAGE III-ISS and correlative measurements are selected by finding the pair of profiles that has the closest geographic distance within a given time interval. The criteria used for finding coincidence varies for different validation studies to get a sufficient number of coincident events for all datasets. In order to obtain enough coincidences, the criteria used for comparison between ACE-FTS and SAGE III-ISS are less than ±5° in latitude, less than ±10° in longitude, and less than ±4 hours in time. Criteria used to find coincidence events between SAGE III-ISS and lidar/ozonesonde data are less than ±5° in latitude, less than ±10° in longitude, and less than ±24 hours in time (Rong et al., 2009). In order to get sufficient comparisons in the Southern Hemisphere the criteria are expanded to less than ±10° in latitude, less than ±20° in longitude, and less than ±10 hours in time. The broad criteria could result in multiple coincidences for a single SAGE III-ISS profile. In the case of multiple matches, the coincident pair that has the smallest time and spatial difference is chosen. This process reduces the duplicate coincidence events in the comparisons. The coincident profiles for the two correlative instruments are found, and then the difference between the two coincident profiles are calculated. For statistical analysis, coincident data are screened to reject the profiles with low-quality measurements according to the recommendation provided by each data product's user guide (SAGE III-ISS Data Products User's Guide: https://eosweb.larc.nasa.gov/project/sageiii-iss/guide/DPUG-G3B-2-0.pdf). Therefore, part of the data record is removed and this decreases the total amount of coincident pairs in our comparisons. (Hubert, D., et al., 2016). The coincident pair of ozone profiles from the two instruments are linearly interpolated to the SAGE III-ISS altitude grid (Rong et al., 2009; Dupuy et al., 2009).

The average difference between the coincident pairs of profiles at a given altitude are calculated using the Eq. (1):

$$\Delta(z) = \frac{1}{N(z)} \sum_{i=1}^{N} \left[\frac{SAGEIII_i(z) - corr_i(z)}{ref_i(z)} \right] \tag{1}$$

where $\Delta(z)$ refers to the average ozone difference at a given altitude z, $SAGEIII_i(z)$ is the ozone concentration at altitude z for the i'th coincident SAGE III-ISS profile, and $corr_i$ is the corresponding

140 concentration for the correlated comparison instrument for the i'th coincident pair. $N(z)$ is the total number of the coincident measurement pairs at altitude z, and $ref_i(z)$ is the i'th reference at altitude z for calculating the difference. The reference for calculating the absolute difference between the coincident pair equals 1. In the case of calculating the relative difference for each coincident pair, the $ref_i(z)$ is the average of the i'th coincident pair concentration at altitude z (Randall et al., 2003; Smith et al., 2013).

145
$$ref_i(z) = \big(SAGEIII_i + corr_i(z)\big)/2 \qquad (2)$$

For comparisons with the lidars and ozonesondes, the reference is taken as the measurement from the ground-based or balloon instrument. As shown in Eq. (3), the standard deviation of the distribution of the relative difference at altitude z provides the spread in the difference for individual coincident pairs. This provides information of the significance of the bias of the SAGEIII-ISS instrument. This standard deviation also provides

150 a measure of the total uncertainty of the instruments that are used for the comparison (von Clarmann, 2006)

$$\sigma(z) = \sqrt{\frac{1}{N(z)-1}\sum_{i=1}^{N(z)}\big[\big(SAGEIII_i(z) - corr_i(z) - \Delta(z)\big)\big]^2} \qquad (3)$$

The statistical uncertainty of the mean difference, also known as standard error of the mean (SEM), is the quantity that allows the significance of the estimated biases to be judged (Dupuy et al., 2009).

155
$$SEM(z) = \sigma(z)/\sqrt{N(z)} \qquad (4)$$

Larger average differences and uncertainties are expected for comparisons using expanded coincidence criteria, such as those used for the sonde and lidar and Southern Hemisphere ACE-FTS measurements.

3. Results

3.1 Comparison between SAGE III-ISS Solar and Ground-based Lidar Measurements

160
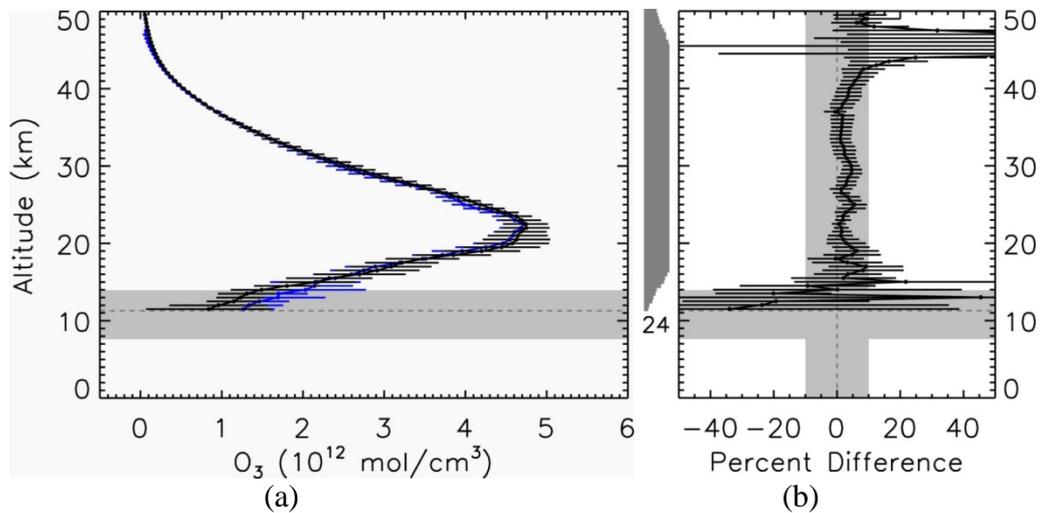
Figure 2(a). The average of all coincident pairs for SAGE III-ISS data and Hohenpeissenberg ozone lidar data for the year June 2017 to May 2018. The average SAGE III-ISS ozone profile is shown as the black line with twice the standard error (2×SEM) shown as black error bars. The average Hohenpeissenberg lidar ozone profile is shown as a blue line with twice the standard error shown as horizontal blue error bars. (b) The average percentage difference between the coincident pairs is shown. The black line indicates the percentage difference, the black horizontal error bars show twice the standard error of the difference, and the vertical grey shading shows the ±10% region. The horizontal grey shading shows the altitude range of the tropopause for both (a) and (b). The horizontal light grey dotted line shows the average altitude of the tropopause height as reported in the SAGE III-ISS data product. The vertical shading on the left side of (b) indicates the variation in the number of coincidences at each altitude (24 total).

One year of data, from June 2017 to May 2018, using the 24 coincident profile pairs between the SAGE III-ISS and the Hohenpeissenberg lidar ozone data, is shown in Figure 2a. The average difference of all coincident pairs

165   for one year of data is calculated and is shown in Figure 2b. The average time difference is 11.8 hours; average latitude difference is 3.4°; average longitude difference is 4.2°; and the average profile distance is 526.6 km. The average percentage difference between the SAGE III-ISS and the Hohenpeissenberg lidar data is less than 5% from 20 to 40 km, and 10% from 16 to 42 km with a very low standard error between 20 km and 40 km, and increasing below and above this region.

(a)   (b)
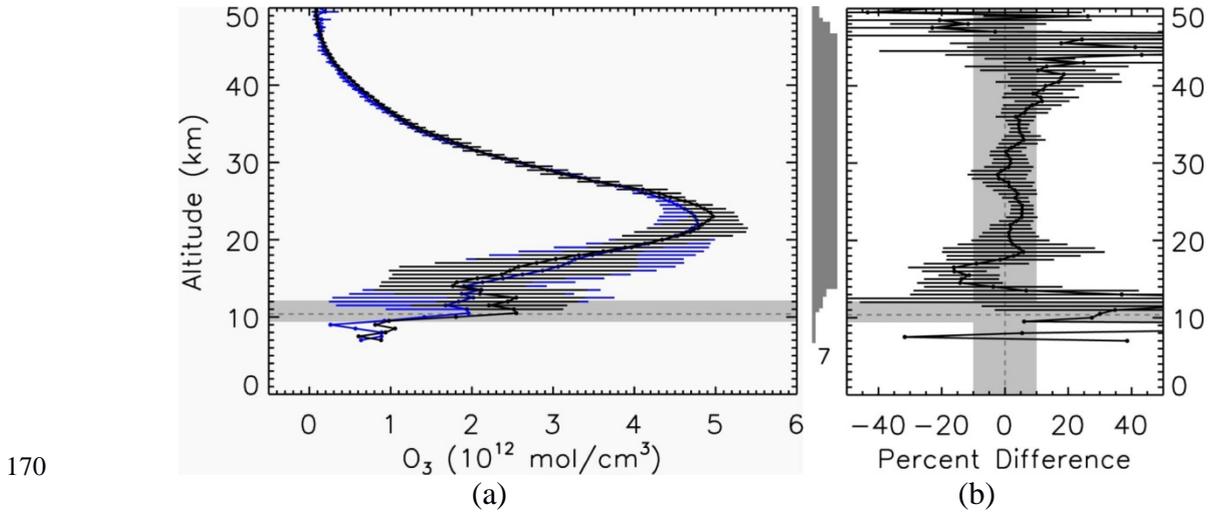
Figure 3. Similar to Figure 2, but for an average difference of coincident pairs of ozone profiles for SAGE III-ISS and Lauder ozone lidar data for the year June 2017 through May 2018.

Similarly, comparisons between the coincident pairs of the SAGE III-ISS and Lauder ozone lidar are shown in Figure 3. There is a total of 7 coincident pairs found within 12.6 hours average time, 2.2° average latitude difference, 3.6° average longitude difference, and 381.5 km average separation distance. The average percentage

175   difference is less than 10% from about 17 to about 37 km with a low standard error between 20 and 40 km.

3.2 Comparison between SAGE III-ISS Solar and Ozonesonde Measurements

The average of 35 coincident ozone profile pairs between SAGE III-ISS and Hohenpeissenberg ozonesondes is compared as shown in Figure 4. Note that the altitude spread of these comparisons are shown as the vertical grey bar. The coincident pairs had an average time difference of 9.7 hours, latitude difference of 3.2°, longitude

180   difference of 4.5°, and a 516.0 km distance. The average ozone percentage differences are found to be less than 10% from about 18 to 30 km. The SAGE III-ISS ozone values show an average positive difference increase above 27 km where uncertainties in the Brewer-Mast ozonesonde measurements rapidly increase (Kerr et al., 1994). The comparison of coincident profile pairs between SAGE III-ISS and the Lauder ozonesonde data is shown in Figure 5. A total of 13 coincident pairs are found from June 2017 to May 2018. The coincident pairs

185   have an average time difference of 10.8 hours, average latitude difference of 1.6°, average longitude difference of 3.3°, and a 329.3 km average distance. The average percentage difference between SAGE III-ISS and Lauder ozone concentrations is less than 10% between 19 and 31 km with a low standard error between about 20 and 30 km.

190   (a)   (b)
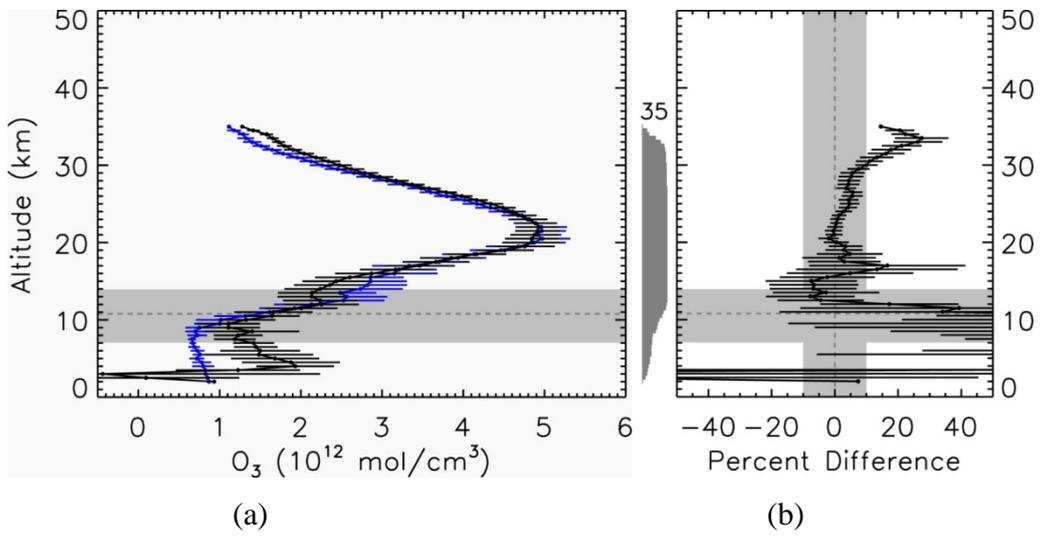
Figure 4. Similar to Figure 2 but for the average difference of coincident pairs for SAGE III-ISS and Hohenpeissenberg ozonesonde profiles obtained for the year June 2017 through May 2018.

(a)   (b)
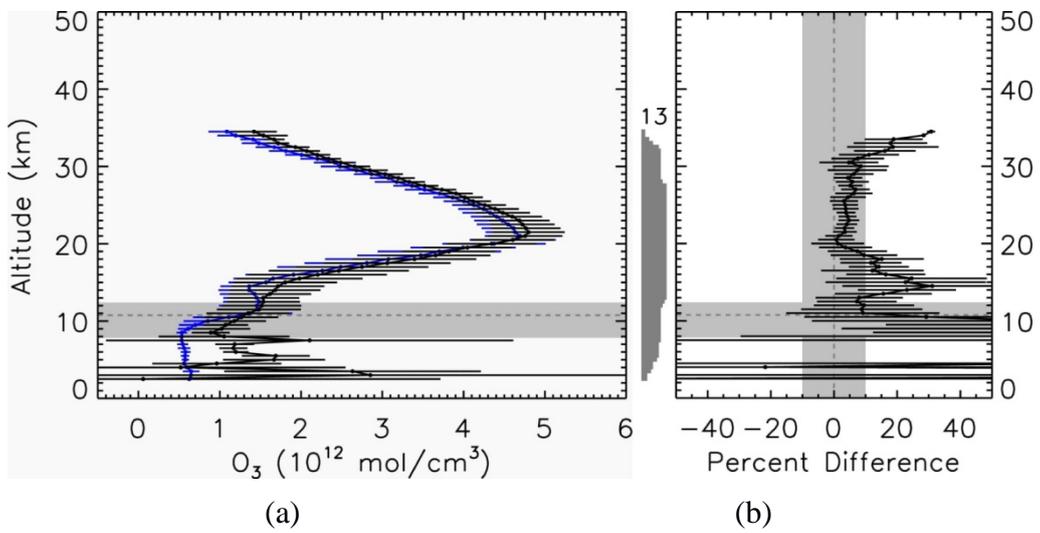
Figure 5. Similar to Figure 2 but for the average difference of coincident pairs for SAGE III-ISS and Lauder ozonesonde profiles obtained for the year June 2017 through May 2018.
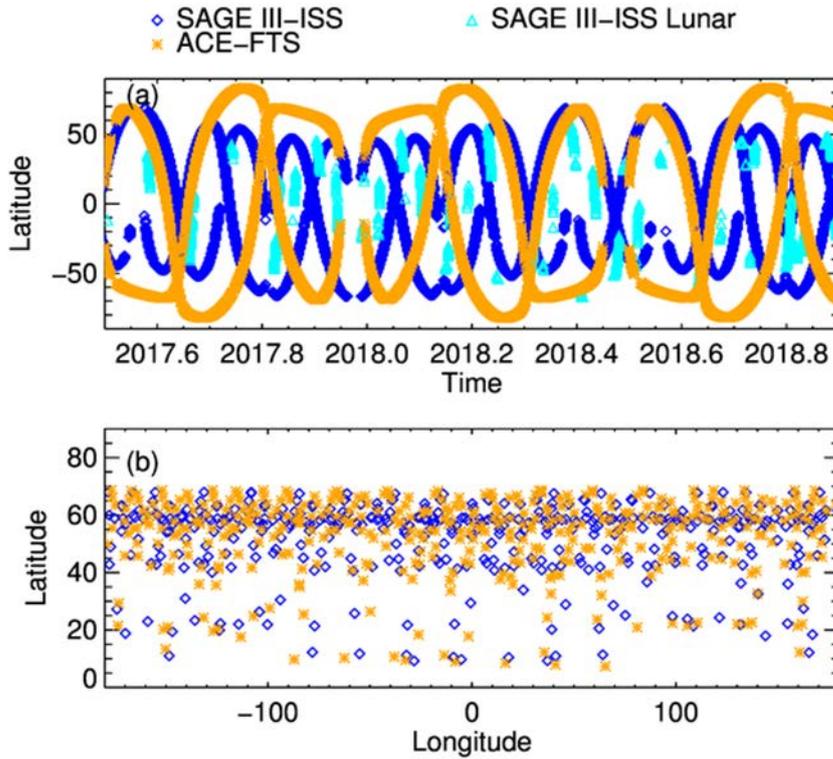
Figure 6. (a) The ACE-FTS and SAGE III-ISS solar and lunar occultation coverage for comparison. (b) The latitude and longitude distribution for coincident events of SAGE III-ISS and ACE-FTS under the criteria of latitude difference less than ±5°, longitude difference less than ±10°, and time difference less than ±4 hours (coincident events could only be found in the Northern Hemisphere).

3.3 Comparisons between SAGE III-ISS Solar and ACE-FTS Measurements

The coincident ozone concentration between the SAGE III-ISS and ACE-FTS is compared in this section. In order to compare with the ozone mixing ratio data from ACE-FTS, the number density data of SAGE III-ISS is converted to volume mixing ratio (ppmv) using the temperature and pressure data reported by SAGE III-ISS. The average coincident ozone profile pairs between the SAGE III-ISS and ACE-FTS are compared for different seasons using SAGE III-ISS level 2 solar data from June 2017 to November 2018. A total of 403 coincident profiles are found using the criteria. Coincident events are mostly located at mid-latitudes and high latitudes in the Northern Hemisphere because of the high inclination of the SAGE III_ISS and ACE-FTS orbits (Dupuy et al., 2009). More than 85% of the coincident SAGE III-ISS and ACE-FTS events are located at latitudes higher than 40° N in this case.

Figures 7 a, c, e, and g show the seasonal average ozone mixing ratio profiles and the standard deviation of their uncertainties for the two instruments in the Northern Hemisphere for JJA (June, July, August, 182 pairs), SON (September, October, November, 119 pairs), DJF (December, January, February, 39 pairs), and MAM (March, April, May, 63 pairs). The SAGE III-ISS average ozone mixing ratio profiles are shown in the blue solid line with the standard deviation of their uncertainties shown as horizontal blue error bars. The ACE-FTS average ozone mixing ratio profiles are shown as the red solid line with the standard deviation of their uncertainties shown as the horizontal red error bars.

Figures 7 b, d, f, and h show the average percentage difference between the two instruments and their standard deviations. The bold black line shows the average percentage difference and the dash-dotted line shows the standard deviation of the percentage difference. The vertical grey regions indicate the ±5% difference region. The mean percentage difference between the two instruments is mostly less than 5% from 20 to 45 km. The comparisons show slightly larger positive differences near 40 km for the DJF, and MAM measurements. The

comparisons show slightly negative differences near 30 km for the SON measurements, and positive differences near 30 km for DJF. Between 20 and 40 km, standard deviations for the percentage differences are less than 5% in JJA and MAM. DJF differences show the largest standard deviation, but are still mostly less than 10% between 20 and 50 km. The standard deviation below 20 km is larger for all seasons with a maximum of 50% in DJF. As shown in Figure 6b, the coincident events between SAGE III-ISS and ACE-FTS are only found in the Northern Hemisphere under the criteria of latitude difference less than ±5°, longitude difference less than ±10°, and time difference less than ±4 hours.
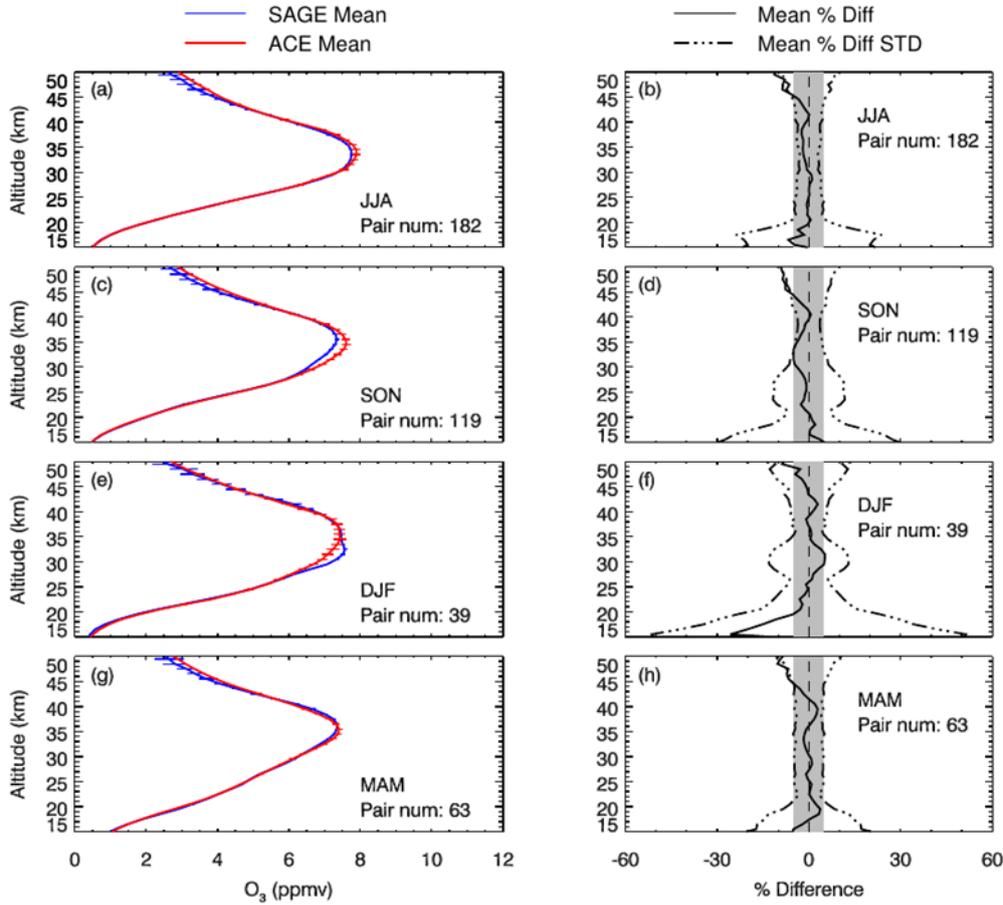
Figure 7.   Seasonal average ozone mixing ratio profile comparisons between coincident SAGE III-ISS and ACE-FTS measurements for the Northern Hemisphere criteria that are described in Figure 6.

A wider criteria of latitude difference less than ±10°, longitude difference less than ±20°, and time difference less than ±10 hours are used to find four seasonal coincident events between the SAGE III-ISS and ACE-FTS in the Southern Hemisphere, and a total of 301 pairs of coincident profiles are found. Similar to Figure 7, Figures 8 a, c, e, and g show the seasonal average ozone mixing ratio profiles and the standard deviation of their uncertainties for the coincident events of the two instruments in the Southern Hemisphere for JJA (144 pairs), SON (58 pairs), DJF (94 pairs), and MAM (5 pairs).

Figure 8 b, d, f, h show that the mean percentage difference between the two instruments is less than 5 % from 20 to 45 km for SON and DJF. The comparison for JJA shows less than 10 % difference between 20 and 50 km with slightly larger positive differences near 30 and 40 km. The comparison for MAM shows less than 5 % difference between 25 and 45 km.   Between 25 and 45 km, standard deviations for the percentage difference are mostly less than 10 % in SON and DJF. Results in JJA and MAM show the largest standard deviation, but still mostly less than 20 % between 20 and 50 km. The standard deviation below 20 km is larger for all seasons with a maximum as large as 60 % in MAM.
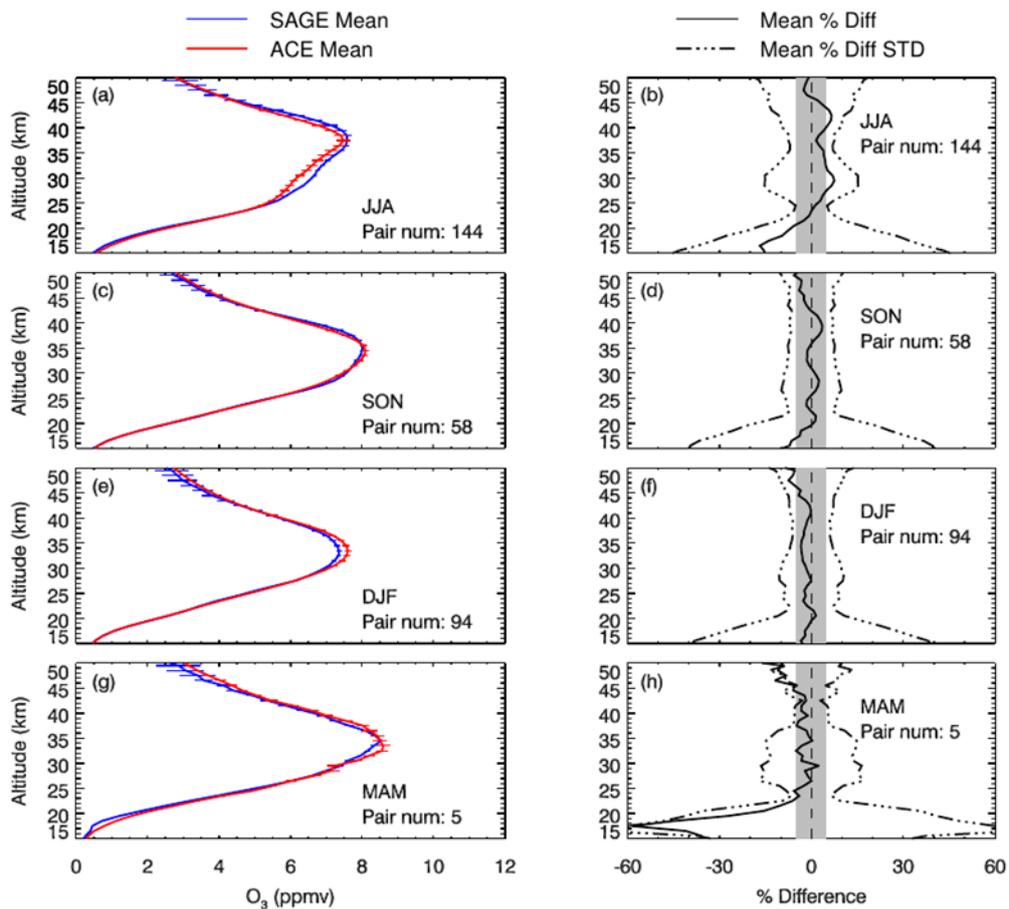
Figure 8. Seasonal average ozone mixing ratio profile comparisons between coincident SAGE III-ISS and ACE-FTS measurements for the Southern Hemisphere under the criteria of differences of latitude less than ±10°, longitude less than ±20°, and time less than ±10 hours.

250
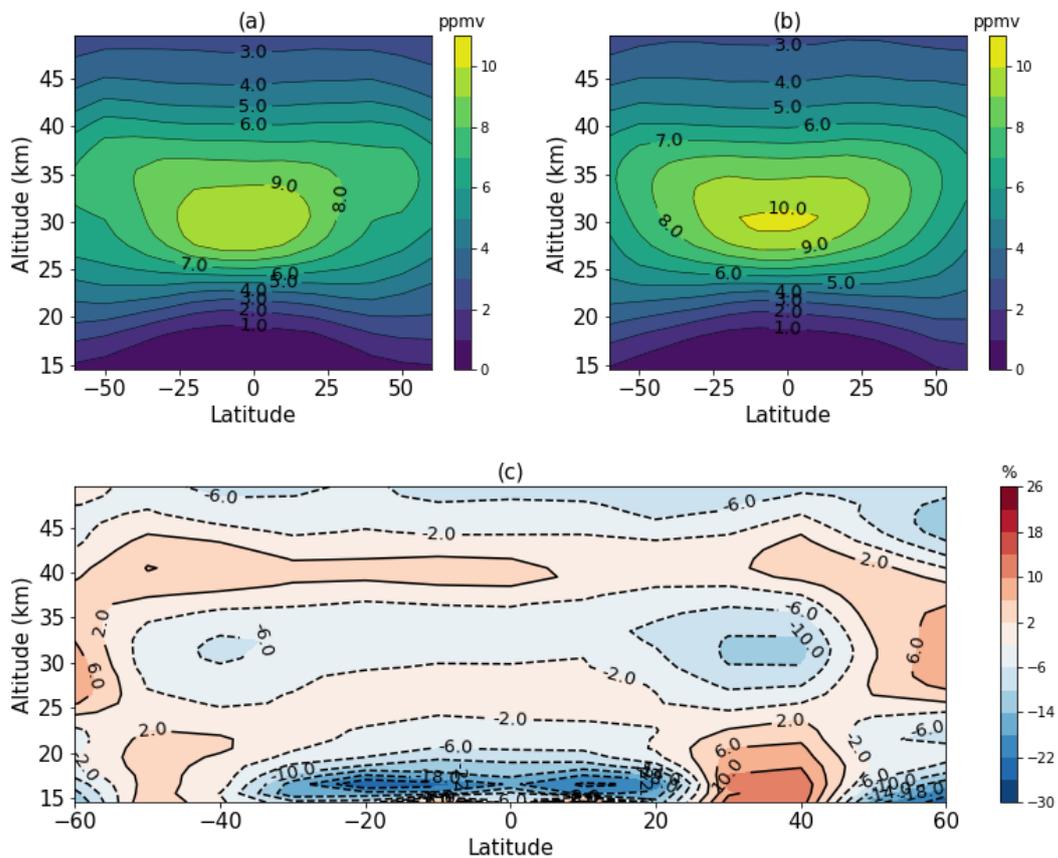
255   The zonal mean ozone mixing ratios from 15 to 50 km for SAGE III-ISS and ACE-FTS are calculated using 10 latitude bins from 60° N to 60° S. Results are shown in Figure 9a and b. The maximum ozone mixing ratios located at about 32 km in the tropical region with maximum mixing ratios larger than 9.8 ppmv are shown for both SAGE III-ISS and ACE-FTS. Figure 9c indicates that SAGE III-ISS zonal average ozone mixing ratios are generally less than ACE-FTS throughout the tropical stratosphere with an exception near 40 km. The differences

260   are mostly less than 5 % except close to the tropical tropopause area, which is most likely impacted by cirrus clouds since they occur more frequently near the tropical tropopause (Nazaryan, H., et al., 2008).

3.4 Comparison between SAGE III-ISS Lunar and Lauder ozonesonde and ACE-FTS profiles
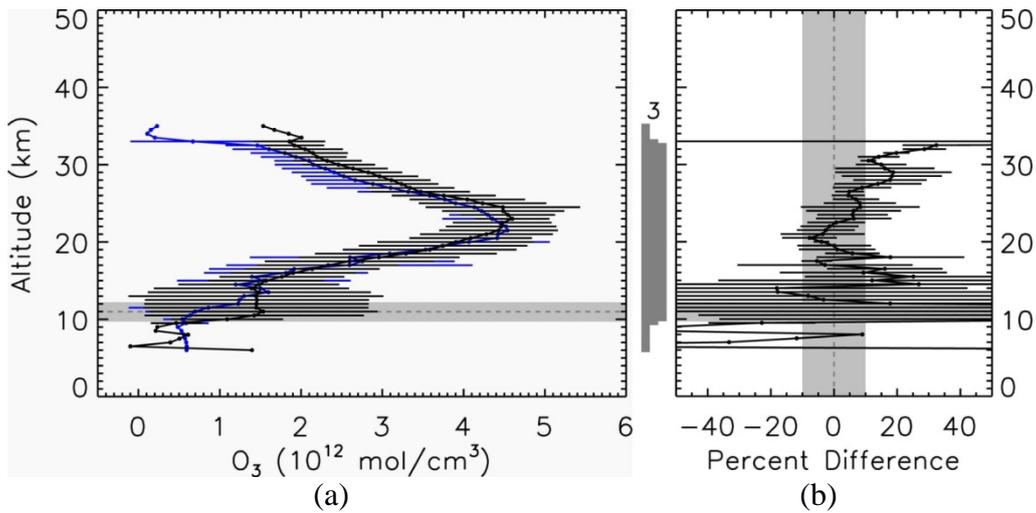
Figure 10. Similar to Figure 2 but for the average difference of coincident pairs for SAGE III-ISS lunar occultation measurements and Lauder ozonesonde profiles obtained for the year June 2017 through May 2018.

265

The coincident lidar, ozonesonde, and ACE-FTS ozone profiles are compared with SAGE III-ISS Lunar ozone profiles. SAGE III/ISS lunar observations are taken much less frequently than solar observations. Consequently, only a few coincidences are obtained within the previously defined criteria, including 3 with Lauder ozonesonde profiles, 7 with ACE-FTS, and fewer than 3 with the other instruments (whose comparisons are not shown).

270
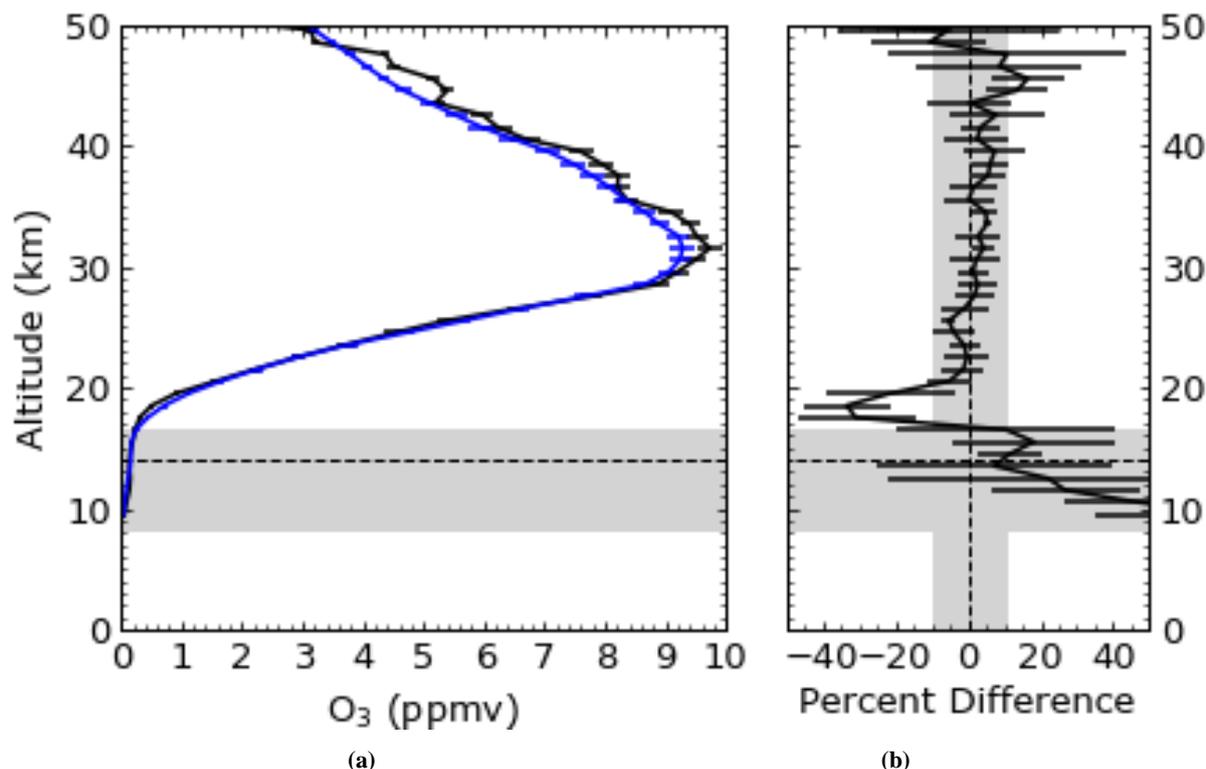
Figure 11. Similar to Figure 2, but for average difference between SAGE III-ISS lunar occultation measurements and the ACE-FTS ozone. Seven comparisons between the SAGE III-ISS lunar and ACE-FTS measurements are shown.

Figure 10 shows a comparison between SAGE III-ISS and Lauder ozonesonde data taken within an average of 7.2 hours of each other, with an average latitude difference of 2.1°, longitude difference of 5.4°, and spatial difference of 508.6 km. The percentage difference between the coincident pairs is less than 10% between approximately 19 and 27 km. The average ozone concentration difference between SAGE III-ISS lunar and

275   ACE-FTS is shown in Figure 11. The average difference between the two data sets is less than 10% with a standard deviation of less than 5% between 20 and 45 km.

4 Conclusions

This paper represents an early effort to provide validation of upper tropospheric and stratospheric ozone measurements from SAGE III-ISS to the broad science-user community. It goes a long way to verify the

280   performance of the SAGE III-ISS satellite instrument, and its capability for providing reliable atmospheric ozone profile measurements. Coincidence measurements from the first year of ozone data provided by SAGE III-ISS are compared with ozone profiles measured by ground-based lidars and ozonesondes. The average differences of ozone concentration measured by SAGE III-ISS and Hohenpeissenberg lidar are less than 10% between 16 and 42 km and less than 5% between 20 and 40 km. The comparisons between the SAGE III-ISS

285   and Lauder lidar ozone measurements are less than 10% between 17 and 37 km. The results of comparisons between SAGE III-ISS and Hohenpeissenberg ozonesondes are mostly less than 10% between 18 and 30 km. When compared with Lauder ozonesondes, the average differences are less than 10% between 19 and 31 km. The average ozone concentration differences between SAGE III-ISS and ACE-FTS are mostly less than 5% between 20 and 45 km in both Northern and Southern Hemispheres during different seasons over the period

290   June 2017 to November 2018. In summary, more than 700 coincident ozone profile pairs are used for the comparisons in this paper, and the results show that SAGE III-ISS is capable of providing ozone profile

measurements that are consistent with another satellite instrument, as well as ground based lidars and ozonesondes developed for such validation measurements. Although there are significantly fewer lunar coincidences available, early results suggest that the lunar ozone measurements agree well with ozonesondes and ACE-FTS. It suggests that SAGE III-ISS ozone data compare well with a number of correlative measurements and given a reasonable lifetime should be used for stratospheric trend and recovery studies as well as research on the impact of ozone on climate variation studies. The authors will continue these comparisons into the near future including more NDACC and other ozone measurements as well as new versions of SAGE III-ISS level 2 data when they become available.

5 Data availability

The satellite ozone profile data used in this work were obtained from:

- SAGE III-ISS v5.1 (available at: https://fpd.larc.nasa.gov/sage-iii.html)

-ACE-FTS v3.5/3.6 (available at: https://database.scisat.ca/level2/ace_v3.5_v3.6/)

The ground-based lidar and ozonesonde ozone profile data were obtained from the NDACC Data Host Facility (http://www.ndacc.org)

Author contribution: Dr. McCormick formulated the overarching research goals. Dr. Hill compared the ozone profiles from SAGE III-ISS with coincident ozone profiles obtained from lidar and sondes. Dr. Lei compared the SAGE III-ISS and ACE-FTS ozone profiles. Dr. Lei wrote the initial draft with contributions from all co-authors. All authors reviewed the manuscript and Dr. McCormick provided the final manuscript for submission.

Acknowledgments

We would like to thank the NASA Langley Research Center (NASA-LaRC) Data Archive Center for providing the SAGE III-ISS solar and lunar occultation data. The ground-based lidar and ozonesonde data used in this publication were obtained from the Hohenpeissenberg Meteorological Observatory, German National Meteorological Hohenpeissenberg, Germany, and the National Institute of Water & Atmospheric Research (NIWA), Lauder, New Zealand, as part of the Network for the Detection of Atmospheric Composition Change (NDACC). The Atmospheric Chemistry Experiment (ACE), also known as SCISAT, is a Canadian-led mission mainly supported by the Canadian Space Agency. We want to thank the ACE team for providing the ACE-FTS ozone data used in this work. This work was partially supported by the National Oceanic and Atmospheric Administration- Cooperative Science Center for Earth System Sciences and Remote Sensing Technologies (NOAA-CESSRST) under the Cooperative Agreement Grant #: NA16SEC4810008. The statements contained within the manuscript/research article are not the opinions of the funding agency or the U.S. government, but reflect the author's opinions.

References

Bernath, P. F., McElroy, C. T., Abrams, M. C., Boone, C. D., Butler, M., Camy-Peyret, C., Carleer, M., Clerbaux, C., Coheur, P. F., Colin, R., DeCola, P., DeMazíere, M., Drummond, J. R., Dufour, D., Evans, W. F. J., Fast, H., Fussen, D., Gilbert, K., Jennings, D. E., Llewellyn, E. J., Lowe, R. P., Mahieu, E., McConnell, J. C., McHugh, M., McLeod, S. D., Michaud, R., Midwinter, C., Nassar, R., Nichitiu, F., Nowlan, C., Rinsland, C. P., Rochon, Y. J., Rowlands, N., Semeniuk, K., Simon, P., Skelton, R., Sloan, J. J., Soucy, M.-A., Strong, K., Tremblay, P., Turnbull, D., Walker, K. A., Walkty, I., Wardle, D. A., Wehrle, V., Zander, R., and Zou, J.:

Atmospheric Chemistry Experiment (ACE): mission overview, Geophys. Res. Lett., 32, L15S01, doi:10.1029/2005GL022386, 2005.

Bodeker, G.E., Boyd, I.S., and Matthews, W.A.: Trends and variability in vertical ozone and temperature profiles measured by ozonesondes at Lauder, New Zealand: 1986-1996, J. Geophys. Res., 103(D22), 28661-28681, 1998.

Boone, C. D., R. Nassar, K. A. Walker, Y. Rochon, S. D. McLeod, C. P. Rinsland, and Bernath, P. F.: Retrievals for the atmospheric chemistry experiment Fourier-transform spectrometer, Appl. Optics, 44 (33), 7218–7231, doi:10.1364/ao.44.007218, 2005.

Bourassa, A. E., Degenstein, D. A., Randel, W. J., Zawodny, J. M., Kyrölä, E., McLinden, C. A., Sioris, C. E., and Roth, C. Z.: Trends in stratospheric ozone derived from merged SAGE II and Odin-OSIRIS satellite observations, Atmos. Chem. Phys., 14, 6983–6994, doi:10.5194/acp-14-6983-2014, 2014.

Bovensmann, H., Burrows, J. P., Buchwitz, M., Frerick, J., Noel, S., Rozanov, V. V., Chance, K. V., and Goede, A. P. H.: SCIAMACHY: Mission objectives and measurement modes, J. Atmos. Sci., 56, 127–150, doi: 10.1175/1520-0469(1999)056<0127:SMOAMM>2.0.CO;2, 1999.

Damadeo, R. P., Zawodny, J. M., Thomason, L. W., and Iyer, N.: SAGE version 7.0 algorithm: application to SAGE II, Atmos. Meas. Tech., 6, 3539–3561, doi:10.5194/amt-6-3539-2013, 2013.

Dupuy, E., Walker, K. A., Kar, J., Boone, C. D., McElroy, C. T., Bernath, P. F., Drummond, J. R., Skelton, R., McLeod, S. D., Hughes, R. C., Nowlan, C. R., Dufour, D. G., Zou, J., Nichitiu, F., Strong, K., Baron, P., Bevilacqua, R. M., Blumenstock, T., Bodeker, G. E., Borsdorff, T., Bourassa, A. E., Bovensmann, H., Boyd, I. S., Bracher, A., Brogniez, C., Burrows, J. P., Catoire, V., Ceccherini, S., Chabrillat, S., Christensen, T., Coffey, M. T., Cortesi, U., Davies, J., De Clercq, C., Degenstein, D. A., DeMazière, M., Demoulin, P., Dodion, J., Firanski, B., Fischer, H., Forbes, G., Froidevaux, L., Fussen, D., Gerard, P., GodinBeekmann, S., Goutail, F., Granville, J., Griffith, D., Haley, C. S., Hannigan, J. W., Höpfner, M., Jin, J. J., Jones, A., Jones, N. B., Jucks, K., Kagawa, A., Kasai, Y., Kerzenmacher, T. E., Kleinböhl, A., Klekociuk, A. R., Kramer, I., Küllmann, H., Kuttippurath, J., Kyrölä, E., Lambert, J.-C., Livesey, N. J., Llewellyn, E. J., Lloyd, N. D., Mahieu, E., Manney, G. L., Marshall, B. T., McConnell, J. C., McCormick, M. P., McDermid, I. S., McHugh, M., McLinden, C. A., Mellqvist, J., Mizutani, K., Murayama, Y., Murtagh, D. P., Oelhaf, H., Parrish, A., Petelina, S. V., Piccolo, C., Pommereau, J.-P., Randall, C. E., Robert, C., Roth, C., Schneider, M., Senten, C., Steck, T., Strandberg, A., Strawbridge, K. B., Sussmann, R., Swart, D. P. J., Tarasick, D. W., Taylor, J. R., Tétard, C., Thomason, L. W., Thompson, A. M., Tully, M. B., Urban, J., Vanhellemont, F., Vigouroux, C., von Clarmann, T., von der Gathen, P., von Savigny, C., Waters, J. W., Witte, J. C., Wolff, M., and Zawodny, J. M.: Validation of ozone measurements from the Atmospheric Chemistry Experiment (ACE), Atmos. Chem. Phys., 9, 287–343, doi:10.5194/acp-9-287-2009, 2009.

Harris, N. R. P., Hassler, B., Tummon, F., Bodeker, G. E., Hubert, D., Petropavlovskikh, I., Steinbrecht, W., Anderson, J., Bhartia, P. K., Boone, C. D., Bourassa, A., Davis, S. M., Degenstein, D., Delcloo, A., Frith, S. M., Froidevaux, L., Godin-Beekmann, S., Jones, N., Kurylo, M. J., Kyrölä, E., Laine, M., Leblanc, S. T., Lambert, J.-C., Liley, B., Mahieu, E., Maycock, A., deMazière, M., Parrish, A., Querel, R., Rosenlof, K. H., Roth, C., Sioris, C., Staehelin, J., Stolarski, R. S., Stübi, R., Tamminen, J., Vigouroux, C., Walker, K. A., Wang, H. J., Wild, J., and Zawodny, J. M.: Past changes in the vertical distribution of ozone–Part 3: Analysis and interpretation of trends, Atmos. Chem. Phys., 15, 9965–9982, doi:10.5194/acp-15-9965-2015, 2015.

Hubert, D., Lambert, J.-C., Verhoelst, T., Granville, J., Keppens, A., Baray, J.-L., Bourassa, A. E., Cortesi, U., Degenstein, D. A., Froidevaux, L., Godin-Beekmann, S., Hoppel, K. W., Johnson, B. J., Kyrölä, E., Leblanc, T., Lichtenberg, G., Marchand, M., McElroy, C. T., Murtagh, D., Nakane, H., Portafaix, T., Querel, R., Russell III,

J. M., Salvador, J., Smit, H. G. J., Stebel, K., Steinbrecht, W., Strawbridge, K. B., Stübi, R., Swart, D. P. J., Taha, G., Tarasick, D. W., Thompson, A. M., Urban, J., van Gijsel, J. A. E., Van Malderen, R., von der Gathen, P., Walker, K. A., Wolfram, E., and Zawodny, J. M.: Ground-based assessment of the bias and long-term stability of 14 limb and occultation ozone profile data records, Atmos. Meas. Tech., 9, 2497–2534, doi: 10.5194/amt-9-2497-2016, 2016.

Kerr, J.B., Fast, H., McElroy, C.T., Oltmans, S.J., Lathrop, J.A., Kyro, E., Paukkunen, A., Claude, H., Koehler, U., Sreedharan, C.R., Takao, T., and Tsukagoshi, Y.: The 1991 WMO International Ozonesonde Intercomparison at Vanscoy Canada, Atmosphere Ocean, 32, No. 4, 685-716, 1994.

Leblanc, T., Sica, R.J., van Gijsel, J.A.E., Godin-Beekmann, S., Haefele, A., Trickl, T., Payen, G., and Gabarrot, F.: Proposed standardized definitions for vertical resolution and uncertainty in the NDACC lidar ozone and temperature algorithms Part 1: Vertical resolution, Atmos. Meas. Tech., 9, 4029-4049, https://doi.org/10.5194/amt-9-4029-2016, 2016.

Leblanc, T., Sica, R. J., van Gijsel, J. A. E., Godin-Beekmann, S., Haefele, A., Trickl, T., Payen, G., and Liberti, G.: Proposed standardized definitions for vertical resolution and uncertainty in the NDACC lidar ozone and temperature algorithms Part 2: Ozone DIAL uncertainty budget, Atmos. Meas. Tech., 9, 4051-4078, https://doi.org/10.5194/amt-9-4051-2016, 2016.

Leblanc, T., Sica, R. J., van Gijsel, J. A. E., Haefele, A., Payen, G., and Liberti, G.: Proposed standardized definitions for vertical resolution and uncertainty in the NDACC lidar ozone and temperature algorithms Part 3: Temperature uncertainty budget, Atmos. Meas. Tech., 9, 4079-4101, https://doi.org/10.5194/amt-9-4079-2016, 2016.

Lucke, R. L., Korwan, D., Bevilacqua, R. M., Hornstein, J. S., Shettle, E. P., Chen, D. T., Daehler, M., Lumpe, J. D., Fromm, M. D., Debrestian, D., Neff, B., Squire, M., Ǩonig-Langlo, G., and Davies, J.: The Polar Ozone and Aerosol Measurement (POAM III) Instrument and Early Validation Results, J. Geophys. Res., 104, 18 785–18 799, doi: 10.1029/1999JD900235, 1999.

Imai, K., Manago, N., Mitsuda, C., Naito, Y., Nishimoto, E., Sakazaki, T., Fujiwara, M., Froidevaux, L., von Clarmann, T., Stiller, G. P., Murtagh, D. P., Rong, P.-P., Mlynczak, M. G., Walker, K. A., Kinnison, D. E., Akiyoshi, H., Nakamura, T., Miyasaka, T., Nishibori, T., Mizobuchi, S., Kikuchi, K. I., Ozeki, H., Takahashi, C., Hayashi, H., Sano, T., Suzuki, M., Takayanagi, M., and Shiotani, M.: Validation of ozone data from the superconducting Submillimeter-Wave Limb-Emission Sounder (SMILES), J. Geophys. Res., 118, 5750–5769, doi:10.1002/jgrd.50434, 2013.

McCormick, M. P., Zawodny, J. M., Veiga, R. E., Larsen, J. C., and Wang, P. H.: An overview of SAGE I and II ozone measurements, Planetary Space Sci., 37, 1567–1586, doi: 10.1016/0032-0633(89)90146-3 , 1989.

McCormick, M. P., Veiga, R. E., and Chu, W. P.: Stratospheric ozone profile and total ozone trends derived from the SAGE I and SAGE II data, Geophys. Res. Lett., 19, 269–272, doi:10.1029/92GL00187, 1992.

Nazaryan, H., McCormick, M. P., and Menzel, W. P.: Global characterization of cirrus clouds using CALIPSO data, J. Geophys. Res., 113, D16211, doi:10.1029/2007JD009481, 2008

Randall, C. E., Rusch, D. W., Bevilacqua, R. M., Hoppel, K. W., Lumpe, J. D., Shettle, E., Thompson, E., Deaver, L., Zawodny, J., Kyrö, E., Johnson, B., Kelder, H., Dorokhov, V. M., KönigLanglo, G., and Gil, M.: Validation of POAM III ozone: Comparison with ozonesonde and satellite data, J. Geophys. Res., 108, 4367, doi:10.1029/2002JD002944, 2003.

Reinsel, G., Weatherhead, E. C., Tiao, G. C., Miller, A. J., Nagatani, R., Wuebbles, D. J., and Flynn, L. E.: On detection of turnaround and recovery in trend for ozone, J. Geophys. Res., 107(D10), doi:10.1029/2001JD000500, 2002.

Rex, M., Salawitch, R. J., von der Gathen, P., Harris, N. R. P., Chipperfield, M. P., and Naujokat, B.: Arctic

385   ozone loss and climate change, Geophys. Res. Lett., 31, L04116, doi:10.1029/2003GL018844, 2004

Rong, P. P., Russell III, J. M., Mlynczak, M. G., Remsberg, E. E., Marshall, B. T., Gordley, L. L., and Lopez-Puertas, M.: Validation of Thermosphere Ionosphere Mesosphere Energetics and Dynamics/Sounding of the Atmosphere using Broadband Emission Radiometry (TIMED/SABER) v1.07 ozone at 9.6 μm in altitude range 15–70 km, J. Geophys. Res., 114, D04306, doi:10.1029/2008JD010073, 2009.

390   Russell, J. M., Gordley, L. L., Park, J. H., Drayson, S. R., Tuck, A. F., Harries, J. E., Cicerone, R. J., Crutzen, P. J., and Frederick, J. E.: The Halogen Occultation Experiment, J. Geophys. Res., 98, 10 777–10 797, doi:10.1029/93JD00799, 1993.

Stratospheric Aerosol and Gas Experiment on the International Space Station (SAGE III/ISS) Data Products User's Guide, Version 2.0 October 2018: https://eosweb.larc.nasa.gov/project/sageiii-iss/guide/DPUG-G3B-2-

395   0.pdf.

Smith, A. K., Harvey, V. L., Mlynczak, M. G., Funke, B., Garcia-Comas, M., Hervig, M., Kaufmann, M., Kyrölä, E., López-Puertas, M., McDade, I., Randall, C. E., Russell III, J. M., Sheese, P. E., Shiotani, M., Skinner, W. R., Suzuki, M., and Walker, K. A.: Satellite observations of ozone in the upper mesosphere, J. Geophys. Res., 118, 5803–5821, doi: 10.1002/jgrd.50445, 2013.

400   Solomon, S.: Stratospheric ozone depletion: a review of concepts and history, Rev. Geophys., 37, 275–316, doi:10.1029/1999RG900008, 1999.

Son, S. W., Polvani, L. M., Waugh, D. W., Akiyoshi, H., et al.: The impact of stratospheric ozone recovery on the Southern Hemisphere westerly jet, Science, 320, 1486–1489, doi:10.1126/science.1155939, 2008.

SPARC/IOC/GAW: Assessment of Trends in the Vertical Distribution of Ozone, WMO - Ozone Research and

405   Monitoring Project Report No. 43, 1998.

Thompson, D. W. J., Solomon, S., Kushner, P. J., England, M. H., Grise, K. M., and Karoly, D. J.: Signatures of the Antarctic ozone hole in Southern Hemisphere surface climate change, Nat. Geosci., 4, 741–749, 2011.

von Clarmann, T.: Validation of remotely sensed profiles of atmospheric state variables: strategies and terminology, Atmos. Chem. Phys., 6, 4311–4320, doi:10.5194/acp-6-4311-2006, 2006.

410   Wang, H.-J., Cunnold, D. M., Trepte, C., Thomason, L. W., and Zawodny, J. M.: SAGE III solar ozone measurements: Initial results, Geophys. Res. Lett., 33, doi:10.1029/2005GL025099, 2006.

Waymark, C., Walker, K. A., Boone, C. D. and Bernath, P. F.: ACE-FTS version 3.0 data set: validation and data processing update in: Proceedings of the ACVE workshop, Frascati, Italy, March 2013, Ann. Geophys., 56, doi:10.4401/ag-6339, 2013.

415   Weber, M., W. Steinbrecht, R. van der A, S. M. Frith, J. Anderson, M. Coldewey-Egbers, S. Davis, D. Degenstein, V. E. Fioletov, L. Froidevaux, D. Hubert, J. de Laat, C. S. Long, D. Loyola, V. Sofieva, K. Tourpali, C. Roth, R. Wang, and J. D. Wild, 2018: Stratospheric Ozone [in "State of the Climate in 2017"]. Bull. Amer. Meteor. Soc., 99 (8), S51-S54, doi:10.1175/2018BAMSStateoftheClimate.I.